The Relationship between Large-Scale Convective Rainfall and Cold Cloud over the Western Hemisphere during 1982–84

PHILLIP A. ARKIN

Climate Analysis Center, National Meteorological Center, NMC/NWS/NOAA, Washington, DC 20233

BERNARD N. MEISNER

Department of Meteorology, University of St. Thomas, Houston, TX 77006

(Manuscript received 4 January 1986, in final form 3 July 1986)

ABSTRACT

Estimates of areal- and time-averaged convective precipitation derived from geostationary satellite imagery using a simple thresholding technique are presented. The estimates are based on measurements of the monthly mean fraction of 2.5° × 2.5° areas covered by clouds whose equivalent blackbody temperature in infrared imagery is below 235 K. The transformation between fractional coverage and rainfall amount is based upon comparisons of fractional coverages using a variety of temperature thresholds and spatial and temporal averaging scales with areal averaged rainfall from the GARP Atlantic Tropical Experiment.

Three-year means of the estimated precipitation for the period December 1981–November 1984 are shown for each of the (3-month) calendar seasons and compared with published descriptions of the long-term seasonal mean rainfall fields. Over the tropical oceans agreement is quite good with no evidence of any systematic errors. Over the Americas, long-term means derived from station observations of rainfall show less extensive areas of heavy rainfall than those derived here, and a slight tendency for lower peak values during the rainy season.

The interannual variability during the 3-yr period is described and compared with station observations of rainfall. The relationship between cloud cover and rainfall in the tropics (30°N–30°S) is found to be similar to that found in previous studies, with a threshold of 235 K giving highest correlations, while observations between 30° and 50° were best correlated with a threshold of 220 K. The large changes in rainfall distribution over South America associated with the 1982–83 ENSO episode and the breaking of the drought in Northeast Brazil during 1984 are clear in the estimates presented here, but the amplitude of the changes is somewhat overestimated. Warm season rainfall observed over the United States is less than the estimates, except near the Gulf of Mexico and southeast United States coast where the degree of overestimation increases away from the coast.

1. Introduction

Tropical convective precipitation, with the attendant release of latent heat, is one of the major forcing mechanisms of the general circulation of the atmosphere. Large-scale anomalies in tropical precipitation are closely associated with global-scale circulation anomalies (Rasmusson and Carpenter, 1982; Horel and Wallace, 1981). A careful monitoring of variations in tropical precipitation is of major importance in any attempt to diagnose the behavior of the global climate system. Knowledge of the actual precipitation averaged over large areas is of potentially great importance for both numerical weather prediction and simulations of the climate using general circulation models (Mintz, 1981). Other applications, such as crop assessment (Strommen et al., 1981) and large basin flood forecasting (Hudlow et al., 1981), can also be easily envisioned.

The task of producing estimates of the areally averaged rainfall for large regions is a challenging one. There are two fundamental methods of measuring rainfall. One is to catch the rain as it falls in some device (i.e., a rain gage) and measure the amount that accumulates. Despite problems associated with the shape of the container, its exposure, the wind and evaporation between measurements, rain gages provide the best available estimates of precipitation at any given point. However, the convective rainfall regimes that dominate large parts of the globe are characterized by small spatial scales (Hudlow, 1979), and a dense network of rain gages is required to produce accurate estimates of areally averaged precipitation. Such a network is simply not possible over the vast majority of the surface of the earth.

The second category of rainfall measurements are those made by some sort of remote sensor. These may be further subdivided into direct (in which information on precipitation-sized droplets is measured) and indirect (in which information on some by-product of the precipitation process, such as clouds, is measured). An example of a direct remote sensing technique is pro-

vided by weather radars. Despite problems such as variations in the reflectivity–rainfall relation, varying droplet size spectra and beam attenuation, among others, good estimates of areally averaged rainfall can be obtained using suitably calibrated digital radars (Hudlow and Patterson, 1979). However, if the radar beam originates from a point on the surface of the earth, it will reach a height above the majority of the precipitation droplets within a few hundred kilometers. This severely limits the area over which any one radar sensor may be used. Even if it were possible to maintain and operate sufficient numbers of radars to cover the world's oceans and remote land areas, the expense would be prohibitive.

Both types of land-based instruments, rain gages and radars, are subject to this difficulty. The obvious solution is to make use of a satellite-based remote sensing device. While both active and passive direct remote sensing devices may be mounted on orbiting spacecraft (Wilheit et al., 1977), the required technology has not yet reached a state in which measurements from such instruments are routinely made and precipitation estimates derived. Satellite-based indirect sensors provide the only currently available means for obtaining estimates of large-scale convective precipitation over the greater portion of the earth, and, in particular, over the tropical oceans on a regular long-term basis.

A wide variety of such indirect techniques has been developed since the advent of meteorological satellite observations. The prototypical approach is to use information provided by visible and/or infrared (IR) imagery regarding the spatial and temporal distribution of cloud top temperature and cloud brightness to deduce the distribution and intensity of precipitation at the surface beneath these clouds. A thorough review of such techniques is provided by Barrett and Martin (1981). While many schemes appear to provide useful estimates of precipitation on a variety of scales, most have features that impede their use in the production of continuous estimates of areally averaged precipitation over long time spans and large regions. In most cases, these are the amounts of manpower and/or computational resources required.

An approach that seems to provide the economies needed to produce estimates on the desired scales but maintains the objectivity afforded by automated processing of digital data is one that uses the aggregate statistical properties of IR cloud top temperatures over large ($>10^4$ km^2) fixed areas. The relationship between such statistics and rainfall in the tropical Atlantic during the GARP Atlantic Tropical Experiment (GATE) was examined by Arkin (1979) and Richards and Arkin (1981). It was shown that 50% to 75% of the variance in areally averaged rainfall accumulations can be explained by a linear function of the mean fraction of the area covered by cloud having equivalent blackbody temperatures (EBBT) colder than thresholds ranging from 220 K to 250 K. Largest values of explained variance were found for a threshold of 235 K and for a spatial averaging area of 2.5° latitude by 2.5° longitude (about 6×10^4 km^2). One of the surprising features of this work was the relative insensitivity of the relationship between fractional cloudiness and rainfall to changes in either the spatial or temporal averaging scale or in the threshold temperature.

These results, together with the results of Kilonsky and Ramage (1976), Griffith et al. (1978), Garcia (1981) and Negri et al. (1984), indicate that the extremely simple process of assigning an appropriate climatological rain rate to each unit area of raining cloud, apparently first proposed by Barrett (1970), exhibits a surprising degree of skill in defining temporally and spatially averaged rainfall on certain scales. While a rainfall estimation technique based on these results is unlikely to provide the resolution and accuracy required for applications such as flash flood forecasting (Hudlow et al., 1981), it certainly has the potential to produce useful large space and long time-scale rainfall estimates. For example, the accuracies and resolutions required to diagnose important short period climate fluctuations (Rasmusson and Arkin, 1981) are obtainable by a threshold technique.

This paper describes the derivation of an estimate of large space- and long time-scale convective precipitation from thresholded GOES IR data. The 3-yr mean annual cycle of monthly rainfall so estimated is compared to long-term mean rainfall over the Americas and the adjacent oceans. The annual and interannual variability in estimated rainfall during the period is compared to that obtained from station rainfall observations over the Americas.

2. Data

As mentioned in section 1, many recent studies of variability in large-scale cloudiness and precipitation have made use of satellite data to some extent. While conclusions based on such data are more clearly valid with respect to cloudiness than precipitation, considerable recent work has shown that over sufficiently large areas, the correlation between the areal extent of cold cloud and areally averaged precipitation is quite high. In this section, we review the evidence that justifies this assertion and describe the data and analyses used in this study.

Arkin (1979) and Richards and Arkin (1981) compared statistics of EBBT derived from geostationary satellite imagery of the GATE A/B array with digital radar estimates of rainfall. Arkin, using hourly imagery, found that the 6-h mean of the fraction of an approximately 2° × 2° area covered by pixels (picture elements) with EBBT less than values ranging from 225 to 255 K was highly correlated with accumulated rainfall during the period. He found similar relationships in all three experimental subperiods. Richards and Ar-

kin (1981) showed that the relationship found by Arkin (1979) was affected by spatial and, to a lesser degree, temporal averaging. Increases in either temporal or spatial averaging scale resulted in improved correlations of the estimates with measured rainfall. The smallest spatial averaging area (0.5° × 0.5°) used was found to exhibit inconsistent results in the different subperiods of GATE, indicating that this scale may fall below the threshold at which useful estimates can be made by a simple thresholding technique. No such effect was found for temporal scale. Correlations between data from individual images and rainfall for the preceding hour were quite high for the larger spatial averaging areas.

These results made it clear that monitoring of the annual and interannual variability in tropical convective precipitation would be possible with estimates derived in this way. Since the data required to produce these estimates were not available on a regular basis, the first step was to develop a routine system for calculating such estimates.

The principal sensor on the U.S. GOES satellites is the Visible-Infrared Spin Scan Radiometer (VISSR). Under normal circumstances, the VISSR produces IR and visible full disk earth images every 30 min. Normally there are two operational satellites, with a combined field of view from about 170°E across the Americas to about 20°W and from about 60°N to 60°S. The IR sensor resolves an element of approximately 64 km^2 and can detect temperature differences of about 1 K. The digital images are processed (Clark, 1983) and stored on the NOAA Central Computer Facility in the VISSR data base. Since each image is retained in operational computer storage for only 24 h and consists of approximately 2×10^6 bytes, compaction is required to produce an archive suitable for calculating precipitation estimates.

Based on the results of Arkin (1979) and Richards and Arkin (1981) and considering the requirements outlined by Rasmusson and Arkin (1981), a temporal averaging scale of one-half month and a spatial scale of 2.5° were chosen. In order to adequately resolve the diurnal cycle, eight images/day are used from each satellite (when available) at 3-h intervals beginning at 0000 GMT. Since imagery from the western GOES satellite is offset by 15 min from the eastern one, images from 15 min before each selected hour (i.e., 2345 GMT for 0000 GMT) are used. All pixels within the area 175°E to 25°W and 50°N to 50°S are sorted into boxes of size 2.5° latitude by 2.5° longitude. When both satellites are available, data west/east of 105°W are obtained from the western/eastern satellite. No overlapping data are used. During periods when only a single satellite is operating, its data are used as far west (or east) as possible. In order to provide the flexibility for possible variation in threshold temperatures, data for each box are sorted into frequency distributions containing 12 classes of width 5 K and four broader classes at the extremes (Table 1). These histograms are summed over half-months separately for each of the eight image times. Thus the basic data set consists of 16-class histograms of EBBT for half-months for each 2.5° × 2.5° box in the domain for each of the eight times of day.

In this paper, data covering the period December 1981 through November 1984 will be presented. It should be noted that although these data are temporally continuous over the majority of this region, there was no western GOES during the 6-month period December 1982–May 1983 and again from August to November 1984. This caused a limitation in coverage during the earlier period to east of 130°–140°W and during the latter to between 55° and 150°W.

Among the potential sources of error in these data are spurious values in the digital data and mislocations introduced by treating the sides of each box as straight lines in satellite coordinates. Examples of the former are occasionally found in the form of pixels for which the gray-scale values are 0 (corresponding to temperatures of >329 K) or 255 (temperatures of <155 K). The circumstances of such values generally indicate that they do not represent actual temperatures, and so they are omitted from the histograms. The latter problem is due to the nonlinear transformation between earth and satellite coordinates. The sides of each box are approximated by straight lines (in satellite coordinates) between the corners, while the true sides are curved. Tests have shown that the typical error introduced in this fashion is the mislocation of <0.5% of the pixels in a tropical box. Elimination of this error would require that the complete transformation between earth and satellite coordinates be carried out for all pixels on the border of the box. This has been found to increase the computational requirements by about two orders of magnitude.

TABLE 1. Limits (in both degrees Kelvin and digital counts) of the classes of the histograms derived from GOES data used in this study.

Class	Temperature limits (K)	Digital count limits
1	>270	<119
2	266–270	119–128
3	261–265	129–138
4	256–260	139–148
5	251–255	149–158
6	246–250	159–168
7	241–245	169–177
8	236–240	178–182
9	231–235	183–187
10	226–230	188–192
11	221–225	193–197
12	216–220	198–202
13	211–215	203–207
14	201–210	208–217
15	191–200	218–227
16	<191	>227

Richards and Arkin (1981) have shown that the linear relationship between areally averaged rainfall and fractional coverage by cold cloud is relatively insensitive to the threshold chosen, and that the coefficients are relatively stable with respect to temporal averaging scale. Both their results and those of Arkin (1979) indicate that the optimum threshold for estimating convective rainfall in 2.5° boxes is 235 K. For this threshold, the slope of the regression relation between fractional cloudiness and rainfall rate is between 2.9 and 3.7 mm h^{-1} while the intercept is 0.1–0.2 mm h^{-1}. For the present application, a constant slope of 3 mm h^{-1} was used everywhere.

Use of a nonzero intercept would result in the estimation of a constant amount of light rain everywhere. Since the physical significance of the positive intercept is questionable, and since its use would not contribute any information regarding spatial or temporal variability, we shall use only the slope of the derived relation in obtaining large-scale estimates.

The rainfall estimates discussed in this paper are referred to as a GOES Precipitation Index (GPI). The GPI is calculated from the product of the mean fractional coverage of cloud colder than 235 K in a 2.5° × 2.5° box, the length of the averaging period in hours and a constant of 3 mm h^{-1}. That is,

$$\mathrm{GPI} = 3F_c t$$

where GPI is in millimeters, F_c is the fractional cloudiness (a dimensionless number between 0 and 1), and t is the length of the period (hours) for which F_c was the mean fractional cloudiness.

An attempt to use a relation derived in the eastern tropical Atlantic to estimate precipitation in other regions must be viewed with caution. The implicit hypothesis is that the convective precipitation process which generates the cold cloud is subject to only relatively small spatial and temporal variations. That is, convection which produces a certain amount of cold cloud for a certain production of rainfall in the eastern tropical Atlantic during summer will have, approximately, the same effect in other areas of the tropical oceans and in other seasons of the year. We also hypothesize that cloudiness and rainfall over continental regions will exhibit a similar relationship during convective regimes. While we do not have statistics to verify that such a universal application of the relationship derived during GATE is in fact justified, the results of Griffith et al. (1980) indicate that one type of indirect rainfall estimate derived for convective rainfall in Florida can be used across the tropical Atlantic and eastern tropical South America. Thus, the reader is asked to bear in mind two important caveats. First, the results presented are applicable only to precipitation produced by deep convection, and second, there will certainly prove to be some seasonal and regional inhomogeneities in the relation between areal extent of cold cloud and rainfall.

3. The annual cycle

The rainfall estimates discussed in this paper must be used with caution. While the general character of the statistical relationship between cloud coverage and convective rainfall on large space- and long time-scales (more cloud implies more rainfall) is probably stable, the smaller-scale components of the precipitation process will certainly exhibit important spatial and seasonal variability. Variation in the low-level moisture and temperature fields will affect the vigor and productivity of convection, and the effects of such variations on cloud top temperatures are not known in detail. Little is known of the large-scale relationship between the microscale details of the precipitation process and the distribution of cold clouds. The GPI can be calculated anywhere equatorward of 50°N and 50°S where geostationary satellite observations are available, but it is expected to provide an accurate estimate of total rainfall only in those areas and seasons that are dominated by convective rainfall. We will emphasize those areas in our analysis.

a. Oceanic rainfall

The 3-yr mean of the fraction of 2.5° × 2.5° boxes covered by cloud with EBBT colder than 235 K for the 3-month seasons December–February (DJF) and June–August (JJA) (Fig. 1) shows that the relationship between fractional cloudiness and rainfall found during GATE appears to be qualitatively valid over broad areas of the tropics. The intertropical convergence zones (ITCZs) and the South Pacific convergence zone (SPCZ) are clearly marked as regions that experience substantially greater frequencies of deep convective cloudiness than other parts of the tropical oceans. The seasonal shifts in convection, both over the oceans and the continents, are also clearly evident. It must be recalled that the months December 1982–May 1983 and August–November 1984 are missing in the central Pacific, and the mean fields there are less meaningful. The months December through May, in particular, are affected by not having been observed during the peak of the anomalous rainfall associated with the 1982–83 El Niño/Southern Oscillation (ENSO) episode (Rasmusson and Wallace, 1983).

These results show that over the oceans the fractional cloudiness begins to increase markedly with latitude poleward of about 25° in the winter, but not the summer, hemisphere. This phenomenon is not observed when a threshold of 220 K is used, indicating that not all cold cloud shows such a latitudinal increase.

The 3-yr mean seasonal rainfall over the tropical oceans, estimated by simply multiplying the fractional coverage by a constant as described in section 2 (Fig. 2), shows a number of interesting spatial features. In the Pacific, a band of rainfall greater than 250 mm is present during each season centered between 5° and

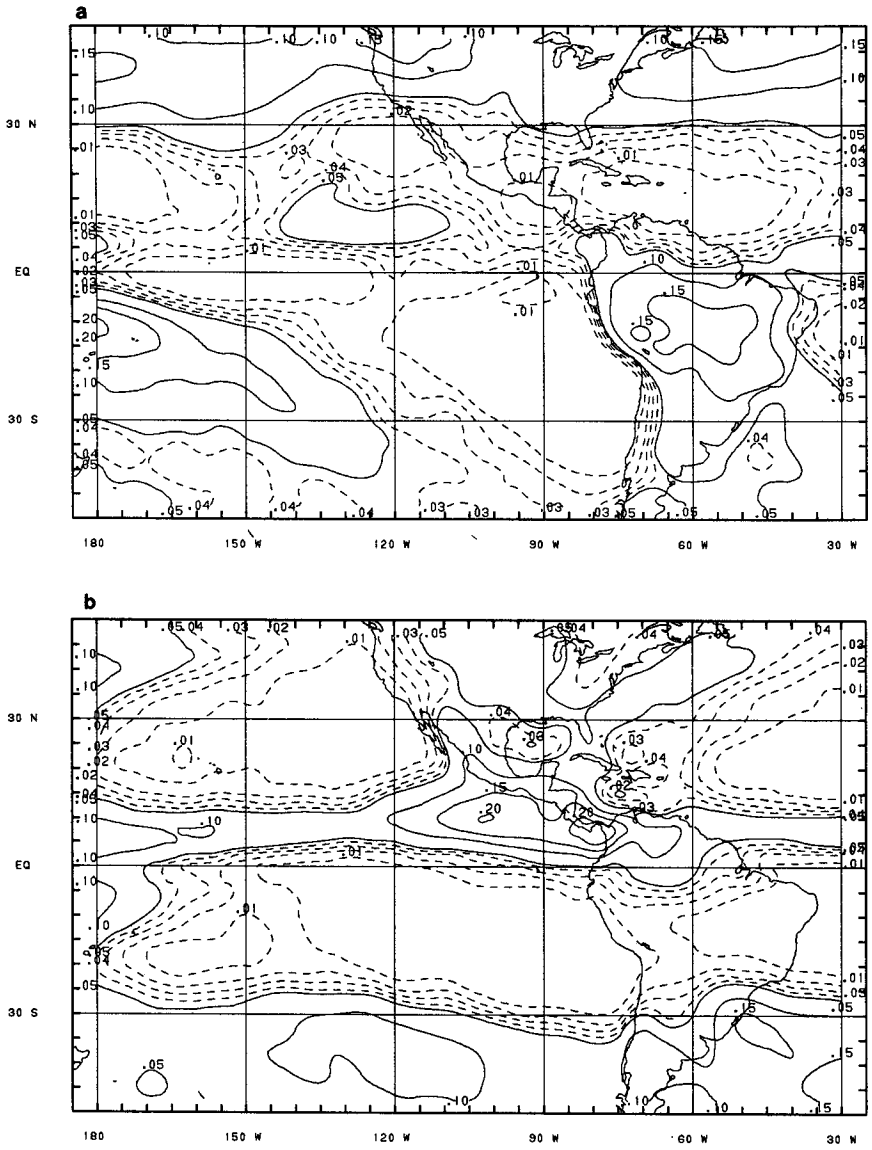

FIG. 1. Three-year mean of the fraction of 2.5° × 2.5° areas covered by pixels with EBBT < 235 K for (a) DJF and (b) JJA. Solid contours at intervals of 0.05, with dashed contours at 0.01 intervals between 0 and 0.05.

10°N. Another such band, somethat farther south during DJF and March–May (MAM), is found in the western Atlantic. These are the ITCZs. Another region of rainfall is centered between 10° and 15°S and the date line, extending toward the southeast. This is the SPCZ (Trenberth, 1976). Regions of relatively low rainfall are found both north and south of the ITCZs in each ocean. The Pacific ITCZ is strongest during JJA, when amounts > 1000 mm are found over an area south of Central America. During this season a relative minimum is found near 130°W, with values increasing to about 750 mm farther west. A similar pattern, although not as intense, is found during September–November (SON), and this feature exhibits much less longitudinal variability during MAM. During the northern winter an opposing pattern is seen, with a maximum found between 120° and 140°W and lower values to the east and west. Values near the date line and just north of the equator exhibit a small relative maximum. Values observed during DJF are considerably below those found during JJA. The SPCZ, on the other hand, exhibits peak values of >1250 mm near its northwestern extremity during SON and DJF, with values about 500 mm less during the other two

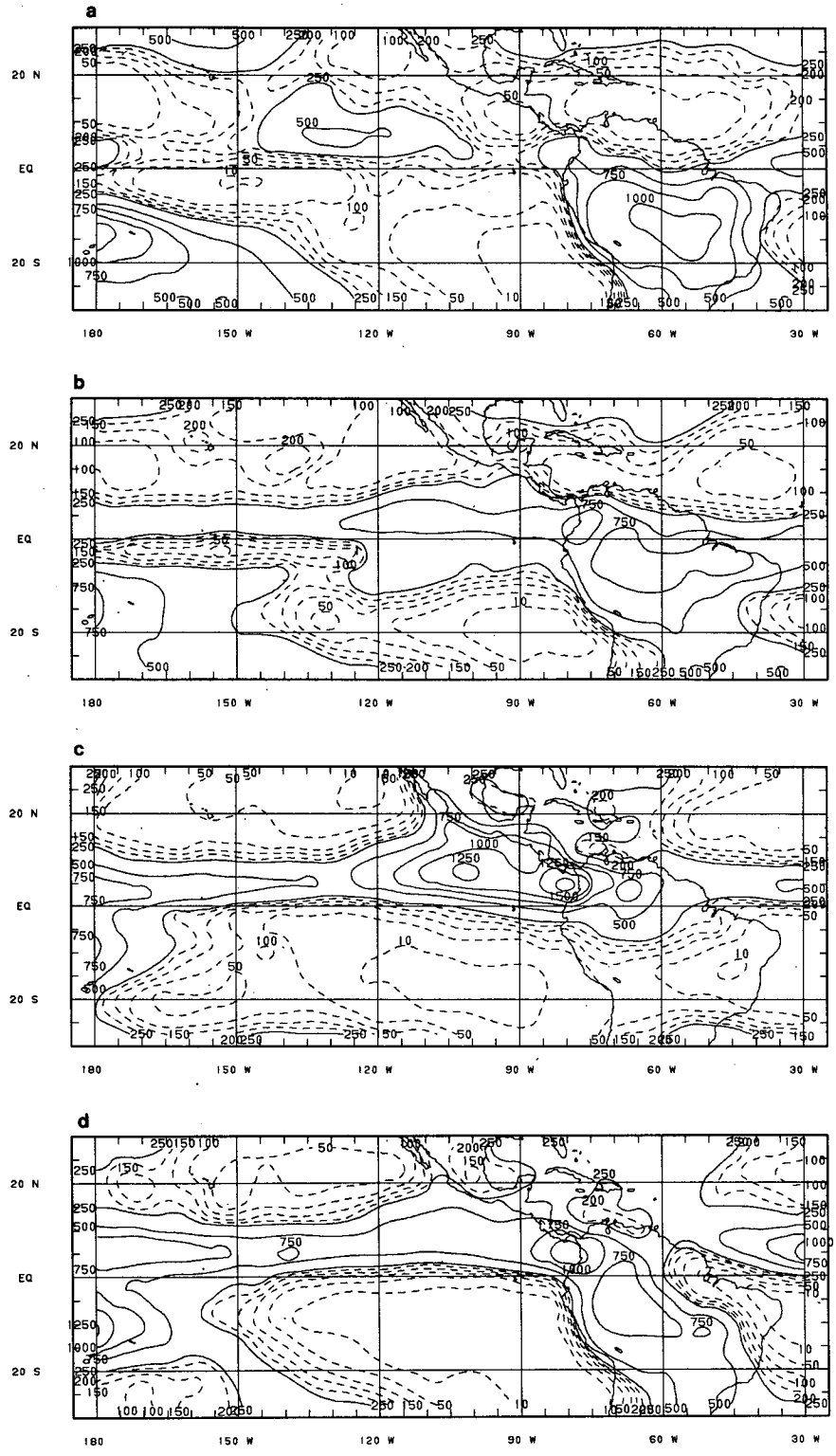

FIG. 2. Three-year mean GOES Precipitation Index (GPI—see text for details) for (a) DJF, (b) MAM, (c) JJA and (d) SON. Solid contours at intervals of 250 mm, with dashed contours at intervals of 50 mm between 50 and 200 mm and a dashed contour at 10 mm.

seasons. The western end of the SPCZ is farthest north, near 10°S, during JJA, and near 15°S during DJF and MAM.

The Atlantic ITCZ exhibits a pronounced seasonal cycle in amplitude, with amounts ranging from >1000 mm during SON to 250–500 mm during MAM and JJA. This feature is farthest north, centered near 5°N, during JJA and SON, and is centered near the equator during MAM. The dry zone in the northern Atlantic is farthest west during DJF, while south of the equator JJA is the driest season. In the South Pacific, SON exhibits the greatest expanse of very dry (<10 mm/season) conditions, while JJA and SON appear to be driest north of the equator.

The results shown in Fig. 2 are in rather good agreement with published estimates of the long-term mean rainfall over these regions. Measurements of oceanic rainfall are extremely difficult to make. Available published maps of long-term mean rainfall have been constructed using compilations of ship observations of current weather and cloudiness, scaled by climatological rainfall rates (Mintz, 1981). This has resulted in a rather wide variation among the published values. Jaeger (1976) shows maps of global monthly precipitation which over the ocean were based on the frequency of precipitation observed by ships and, in the Indian and Pacific Oceans, based on observations at coastal and island stations. Jaeger's maps contained features similar to those discussed here, with similar seasonal variability. The portion of the Pacific ITCZ between about 120° and 150°W had largest amounts during the northern winter, while largest amounts were found in the northern summer farther to the east and west. He found greatest amounts in the SPCZ during the November–February months. He found the Atlantic ITCZ to be farthest north during June–September and farthest south during the northern winter, although he located the center somewhat farther north than is shown here. Jaeger's amounts were typically less than the values in Fig. 2.

Dorman and Bourke (1979, 1981) determined the long-term mean rainfall in the Atlantic and Pacific oceans from an adaptation of a method developed by Tucker (1961). Tucker used land station observations to assign to each observed weather type of the synoptic code a rainfall intensity. Dorman and Bourke (1978) determined that Tucker's coefficients were temperature dependent and developed empirical formulae relating the coefficients to the air temperature. Their maps of seasonal rainfall agree very well with ours. For example, the Atlantic ITCZ is shown to be approximately centered on the equator during MAM. Some of the longitudinal structure found in the Pacific ITCZ in Fig. 2 is not confirmed by Dorman and Bourke, and, in contrast to Jaeger (1976), both the Atlantic and Pacific ITCZs exhibit markedly greater amounts in some areas/seasons than found in our results. In this case, it is possible that some of the difference results from the apparently greater spatial resolution of their results, with the peak values being slightly smeared by the areal averaging in the GPI.

b. South America

Maps of long-term mean rainfall over South America have been produced from compilations of station observations by Hoffman (1975) and Jaeger (1976). It is again noteworthy that, despite reliance on virtually identical sources of data, the long-term mean maps of Hoffman and Jaeger differ in many respects. Clearly, the estimation of the long-term mean monthly or seasonal areal average rainfall is subject to substantial uncertainties, even over continental regions. Their studies show that the long-term mean rainfall over tropical South America has a well-defined annual cycle with maxima near 10°S from October through March and 0°–5°N from April through September. Monthly values of >400 mm are found near 10°S between 50° and 60°W during January–March and near 4°N between 60° and 70°W during June. An axis of substantial rainfall extends NW–SE from October–March, with an extension toward the mouth of the Amazon from January–March. From April–August, the axis of greatest amounts extends roughly E–W near and north of the equator.

Figure 3 shows the 3-yr mean GPI, together with the long-term mean (after Hoffman, 1975), for each season for the region 10°N–30°S and 37.5°–80°W. The results of Hoffman, manually digitized and then plotted on the GPI grid, are also shown. The timing and location of GPI maxima shown here agree well with those in the long-term means of Hoffman. The orientation of the axes of maximum GPI are similar to those in the long-term mean, and largest amounts are found in the summer hemisphere. The GPI gives larger amounts than the published climatologies in the areas of maximum rainfall and maxima in the GPI are further west than those found in Hoffman north of the equator. While many differences in detail are seen in Fig. 3, the qualitative agreement of the large-scale features is as good as could be expected when comparing a 3-yr mean from any source with a long-term mean.

The observed differences between the long-term mean fields and those shown in Fig. 3 result from two factors. Sampling fluctuations due to real interannual variability are certainly present in these data and must have caused some part of the differences. Some aspects of these will be discussed in the following section. The other factor is a systematic error in the methods of rainfall estimation. Note that there are likely to be systematic errors in the published estimates of the long-term mean rainfall derived from station data; this is indicated by the differences found between the works of Hoffman (1975) and Jaeger (1976). A very rough guess at the uncertainty in the long-term monthly mean rainfall in South America, derived from the differences between Hoffman and Jaeger, is 10%–25%.

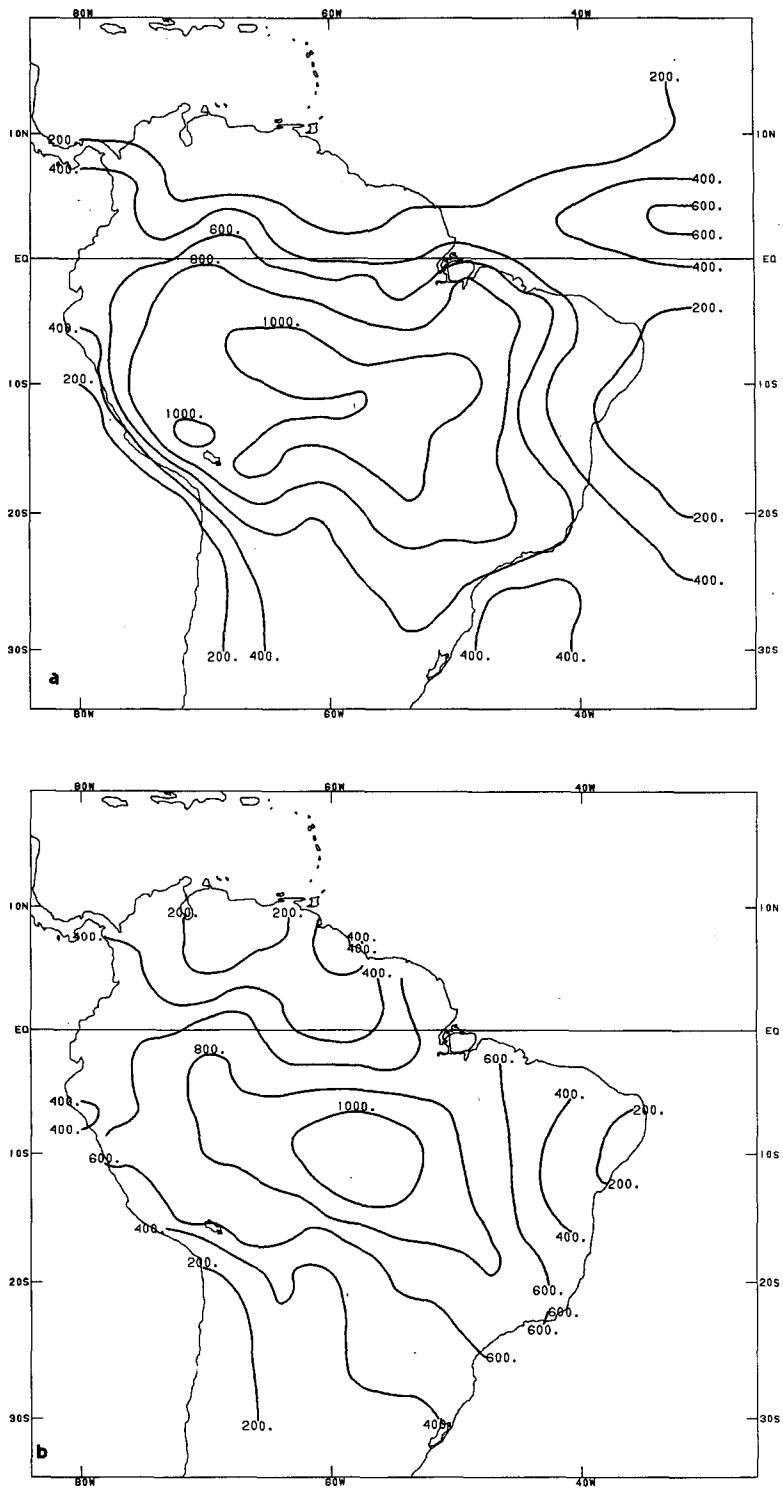

FIG. 3. Three-year mean GPI for (a) DJF, (c) MAM, (e) JJA and (g) SON together with the long-term mean (after Hoffman, 1975) for (b) DJF, (d) MAM, (f) JJA and (h) SON for tropical South America. Contour interval 200 mm.

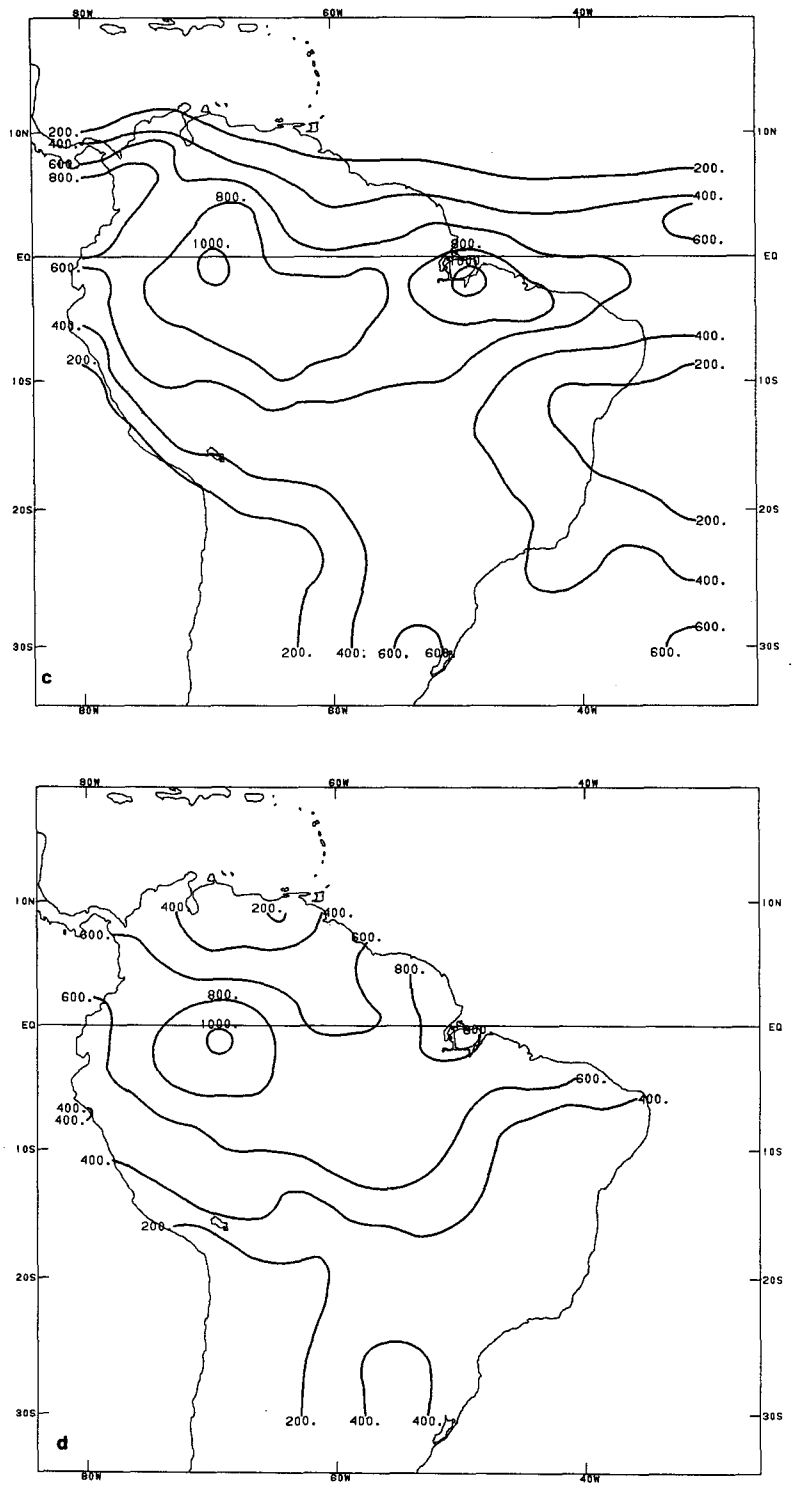

FIG. 3. (*Continued*)

Hoffman's maps were manually digitized to obtain areally averaged rainfall for 2.5° boxes for each month. The climatological annual cycle over South America between 10°N and 30°S (Fig. 4) peaks during January–March and reaches its minimum during August. The GPI (same figure) exhibits an annual cycle with a dis-

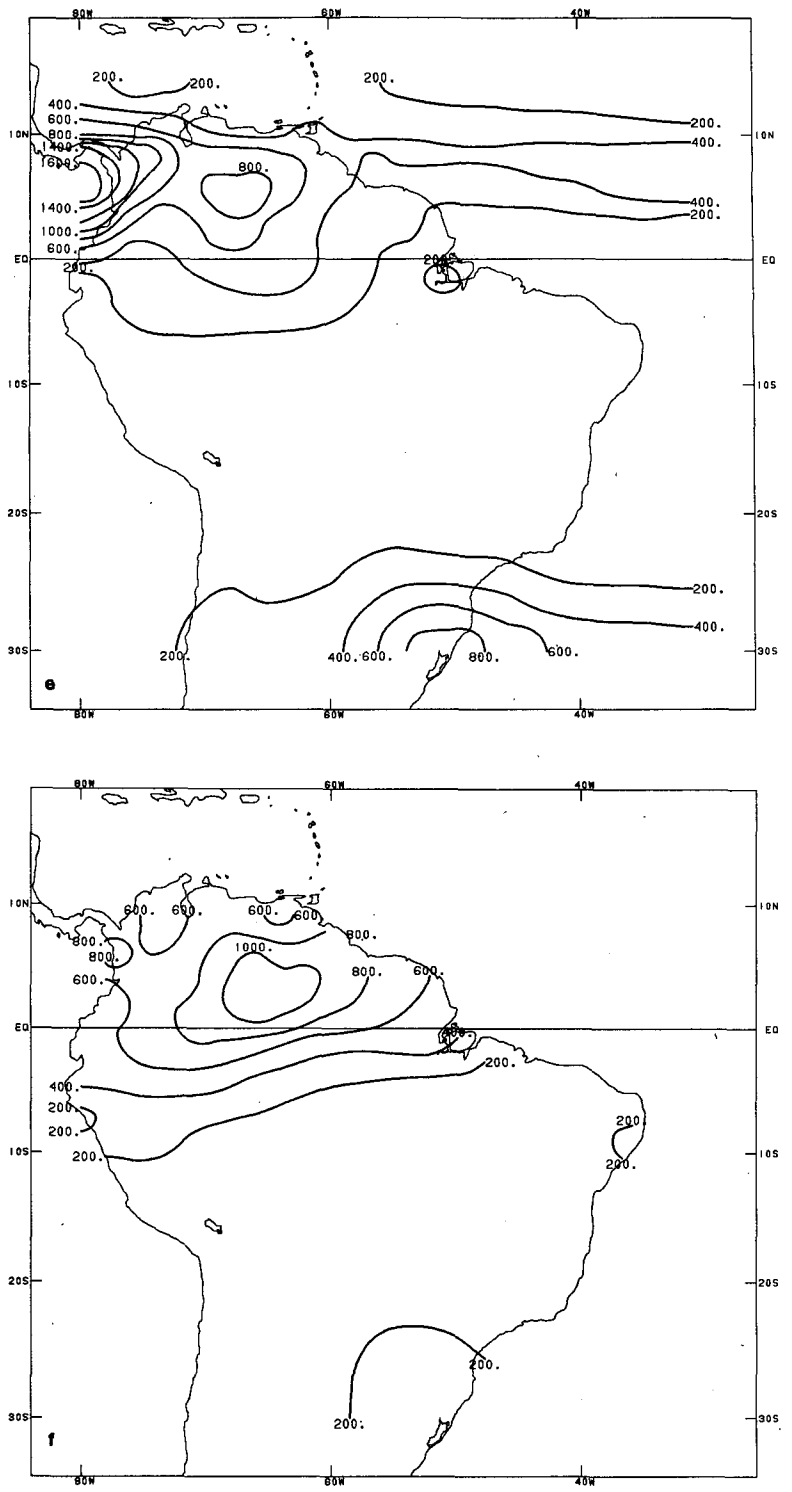

FIG. 3. (*Continued*)

tinctly larger amplitude in each year (greater maxima and lesser minima), but with about the same phasing as the long-term mean. Much of the difference is due to differences in the areal extent of large values between Hoffman's data and the GPI. During the wet season, about twice as many 2.5° areas have a GPI of >300

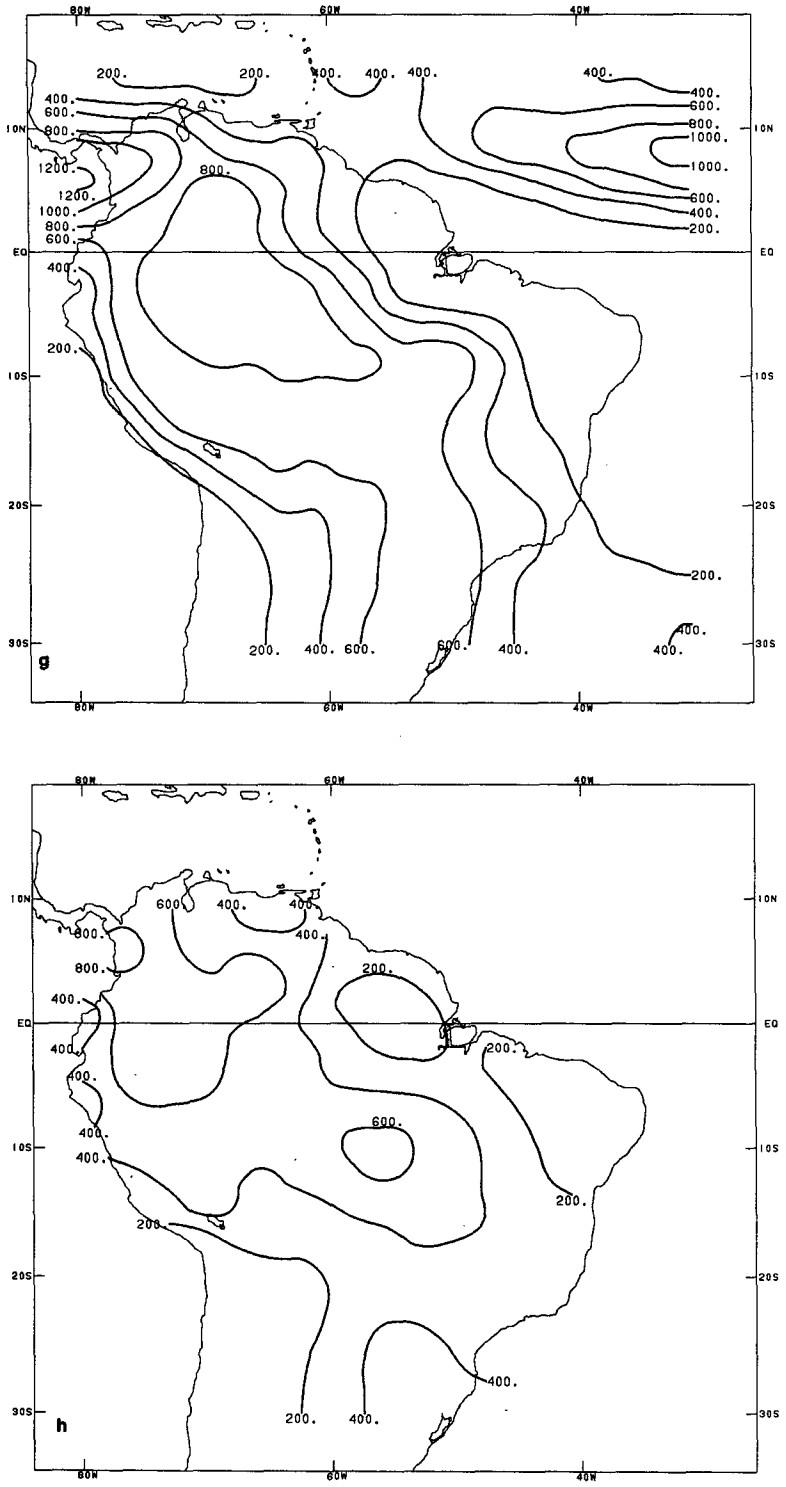

FIG. 3. (*Continued*)

mm/month as have a long-term mean rainfall of that magnitude (Fig. 5a). In contrast, the extent of GPI > 100 mm/month is virtually identical to that of the long-term mean rainfall except during the driest months (Fig. 5b).

One interesting aspect of these results is that the peak

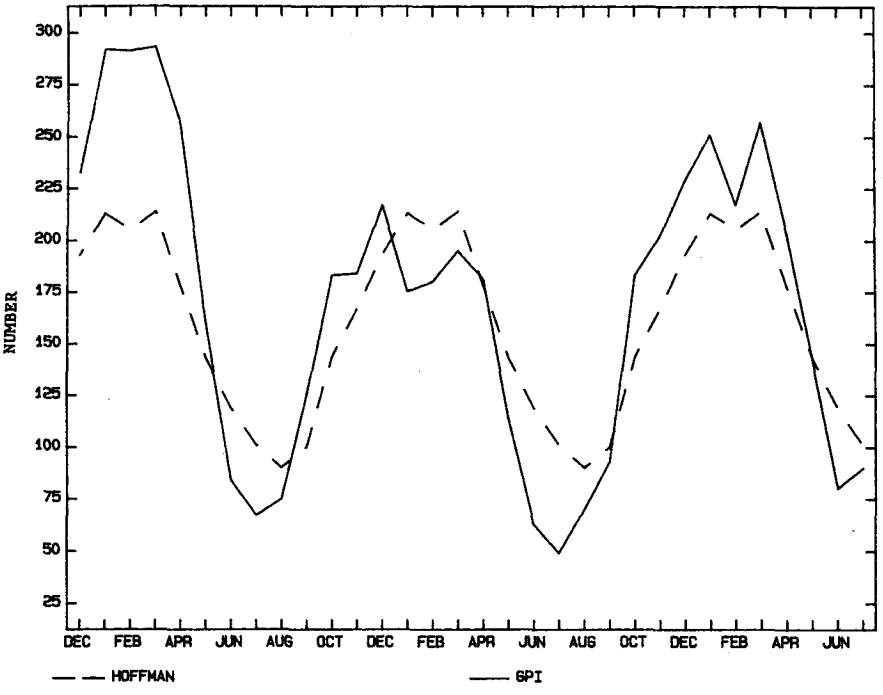

FIG. 4. Time series of monthly GPI (solid) and monthly rainfall from Hoffman (1975) (dashed) averaged over all 2.5° × 2.5° areas in South America between 10°N and 30°S for the period December 1981–November 1984. For August 1984, the averaging is limited to areas west of 65°W, and for September–November 1984, to areas west of 55°W due to the lack of satellite data.

values during a month or season do not differ greatly from the long-term mean, while the areal extent does differ significantly. A characteristic of satellite estimates based solely on the expanse of cold cloud, such as the GPI, is that they are susceptible to "smearing" of maximum values. If this is an important factor in these data, then the actual situation may be one in which peak GPI values would be greater than long-term mean peak values but are in effect spatially smoothed. This interpretation is supported by comparisons with station observations during the period (discussed in section 4). It must be recalled, however, that any convective regime is characterized by large amounts of rainfall in a few areas and little or no rainfall in larger areas; therefore, there is a tendency for isolated station observations to underestimate areal average convective rainfall. While this effect should be reduced by long-term averaging, the network of rainfall-observing stations in South America is probably not sufficiently dense to remove it entirely.

The same explanation cannot be used for the dry season, when GPI estimates are lower than the long-term mean in much of this area. A possible cause of the dry season discrepancy is the fact that the GPI makes no allowance for rain falling from clouds with tops warmer than 235 K. A more detailed comparison between GPI and station observations is presented in section 4, but a complete diagnosis of the errors cannot be performed without much more extensive ground truth data.

c. Central America and Mexico

The mean annual cycle in GPI over Mexico and Central America (Fig. 2) compares well with published results. Largest values of GPI are found during SON and JJA, the latter being the peak season. In all seasons except DJF, an axis of maximum GPI is found south of Central America (the Pacific ITCZ) and decreasing values toward the north. Values during JJA range from >1000 mm in Panama and >500 mm south of about 16°N, and along the southwest coast of Mexico to <250 mm in extreme northeastern Mexico and the northwestern tip of Yucatan. During MAM/SON an axis of minimum GPI is found just south/north of 20°N. During DJF, a minimum is observed along the coasts of Guatemala, El Salvador and Nicaragua.

For the most part, these features closely resemble those of the long-term mean annual cycle given by Jaeger (1976) and Steinhauser (1979). The most important difference between their results and ours is due to the complexity of the rainfall pattern over much of Central America in the maps of Jaeger and Steinhauser and the large spatial scale of the GPI. The large-scale features of the seasonal mean GPI previously discussed are all present with similar timing and amplitude in the long-term mean fields.

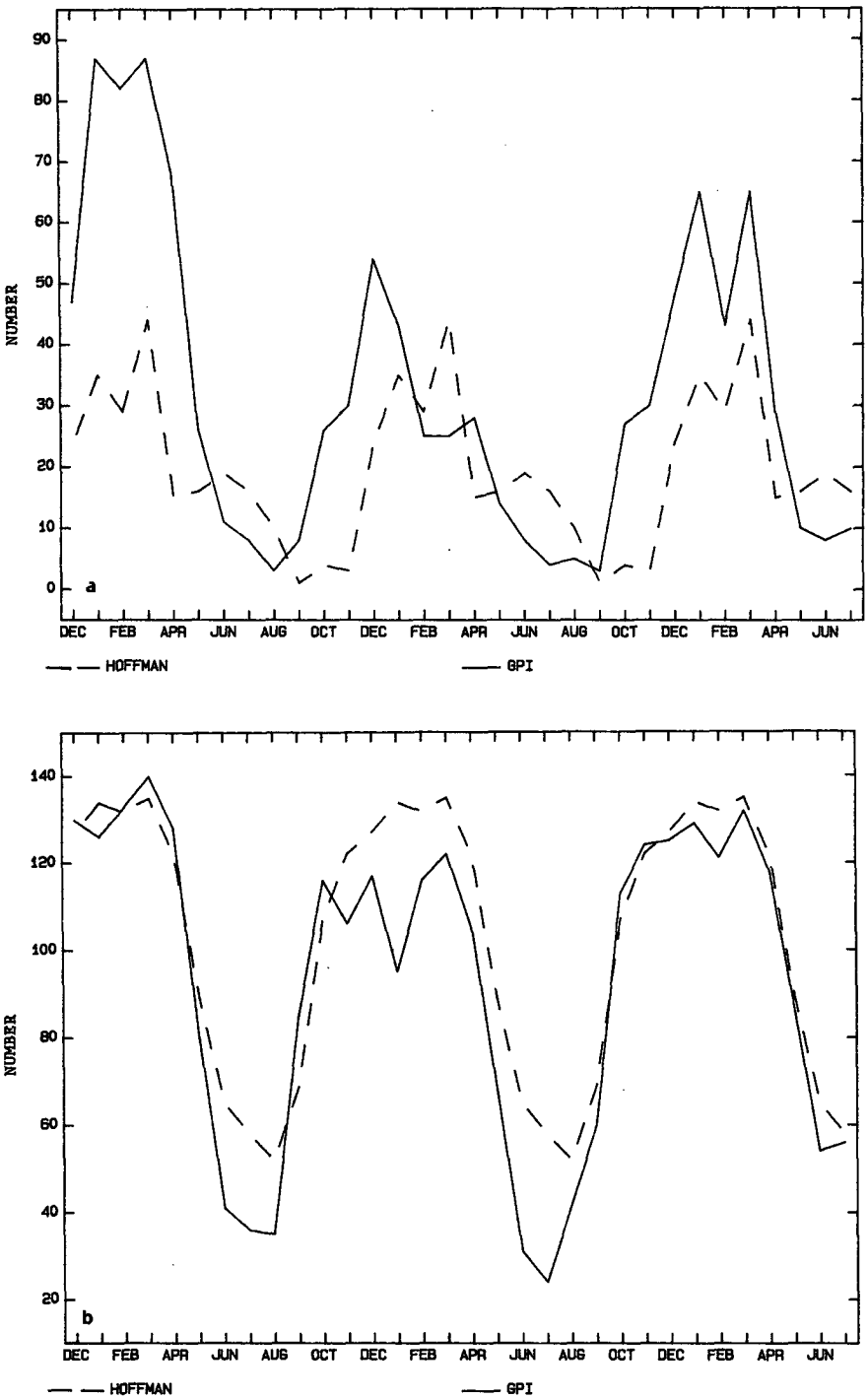

FIG. 5. Time series of the number of 2.5° areas in the spatial domain of Fig. 4 with GPI (solid) and rainfall (dashed—from Hoffman, 1975) (a) >300 mm/month and (b) >100 mm/month.

4. Interannual variability

In this section we will present our findings on the ability of the GPI to reproduce intra- and interannual variations in observed rainfall. A serious obstacle to any such attempt is the scarcity of ground-based observations of rainfall. While there exist a great many rainfall observing stations in most continental regions,

relatively few are widely available. We will first describe a comparison of GPI with all station measurements of rainfall that could be obtained for the first 2 yr of GPI data and then compare variations in GPI over the United States with areal averages computed from a denser network of measurements. Finally, we will discuss the interannual variability of GPI over tropical South America, associated with the 1982–83 ENSO episode.

a. Comparison with station measurements

The GPI estimates were compared with monthly precipitation totals for approximately 550 stations in the Americas, the eastern and central Pacific and the western Atlantic. The precipitation data were either published in *Monthly Climate Data for the World* or the *Weekly Weather and Crop Bulletin,* reported in monthly CLIMAT reports broadcast on the Global Telecommunications System (GTS) or received directly from the observing organization. Not all stations had data for all months of the period. The average number of stations for which data were available in a given month was 465, and these cover approximately 12% of the study area. These precipitation data represent the best coverage one could expect from conventional networks and highlight two of the principal advantages of satellite estimates, namely their complete spatial coverage and the prompt availability. For the period December 1981 through November 1982, there were a total of 3794 station-months (data for one station for one month) of data; for December 1982 through October 1983, 3190 station-months. The data were nearly evenly divided between the tropics and the extratropics. The spatial distribution of stations with available data is shown in Fig. 6.

The rainfall observations from different sources were checked for agreement, and differences were resolved subjectively according to the quality of the various sources. Since the GPI represents an areal average rainfall, some estimate of the areal average rainfall for 2.5° boxes had to be derived from the station observations. It might be argued that the station observations should be used to produce a detailed isohyetal analysis which could then be areally averaged to obtain the appropriate value for each box. However, both the scarcity of the observations and, more importantly, the difficulty in performing the needed analysis caused us to choose a (possibly) less accurate but more reproducible approach. Averages of rainfall for 2.5° boxes were derived by arithmetically averaging all station observations contained in that box.

Spatial correlations (non-area weighted) between GPI and rainfall were computed using all boxes for which we had data for each of the 24 months in the data set. The correlations were calculated for the area from 30°N to 30°S—presumably dominated by convective precipitation throughout the year—as well as the entire 50°N–50°S region. The secular variation in correlation for the two regions (Fig. 7) shows that the smaller region exhibits higher correlations throughout the period. No obvious annual cycle in correlation was observed during the period for either of these areas. The reason for the low correlations during JJA 1982 is not known.

The possibility that the differences in correlation among the two regions result from a greater frequency of nonconvective rainfall in the region from 30° to 50° was tested by comparing fractional coverages, computed using different thresholds (ranging from 215–245 K) with rainfall in the tropics (30°N–30°S) and extratropics (poleward of this region to 50°N and 50°S). The variation of correlation with threshold temperature in the tropics was virtually identical to that found by Arkin (1979), with a broad flat maximum centered near 235–240 K. In the extratropics, on the other hand, the best correlation between fractional coverage and rainfall was found for a threshold of 220 K, with warmer thresholds giving considerably lower correlations. Inspection of maps of fractional coverage in the extratropics (e.g., Fig. 1) showed that considerable extent of cold (<235 K) cloud occurred in regions and times (e.g., the northwestern United States during DJF) that are not characterized by convective precipitation, while a colder threshold of 220 K appeared to eliminate these areas. Even with a threshold of 220 K however, correlations between fractional coverage and rainfall were substantially lower in the extratropics than in the tropics.

b. The United States

As noted in the foregoing, the utility of the GPI in estimating rainfall in the latitudes of the United States is likely to be less than in the tropics. Substantial parts of the year are dominated by nonconvective precipitation, and relatively small-scale surface features may have important effects on rainfall over large parts of the country. However, warm season rainfall over the eastern two-thirds of the country is predominantly convective in nature, and effects due to surface inhomogeneities are probably less there than in the west. Since the spatial distribution of large-scale monthly rainfall over the United States is better known (to the authors at least) than that of any other area for which the GPI is available, we can test our hypothesis that the relationship between GPI and rainfall over the United States will be better during the warm season and in the south and east.

The Climate Divisions (CDs—see Rasmusson et al., 1981) of the United States are a set of 344 areas (each of the 48 contiguous states containing from one to ten areas), each representing an approximately homogeneous region in a climatic sense. Monthly mean temperature and precipitation are obtained for each CD by averaging observations for a selected set of observing stations. Values of monthly mean precipitation are

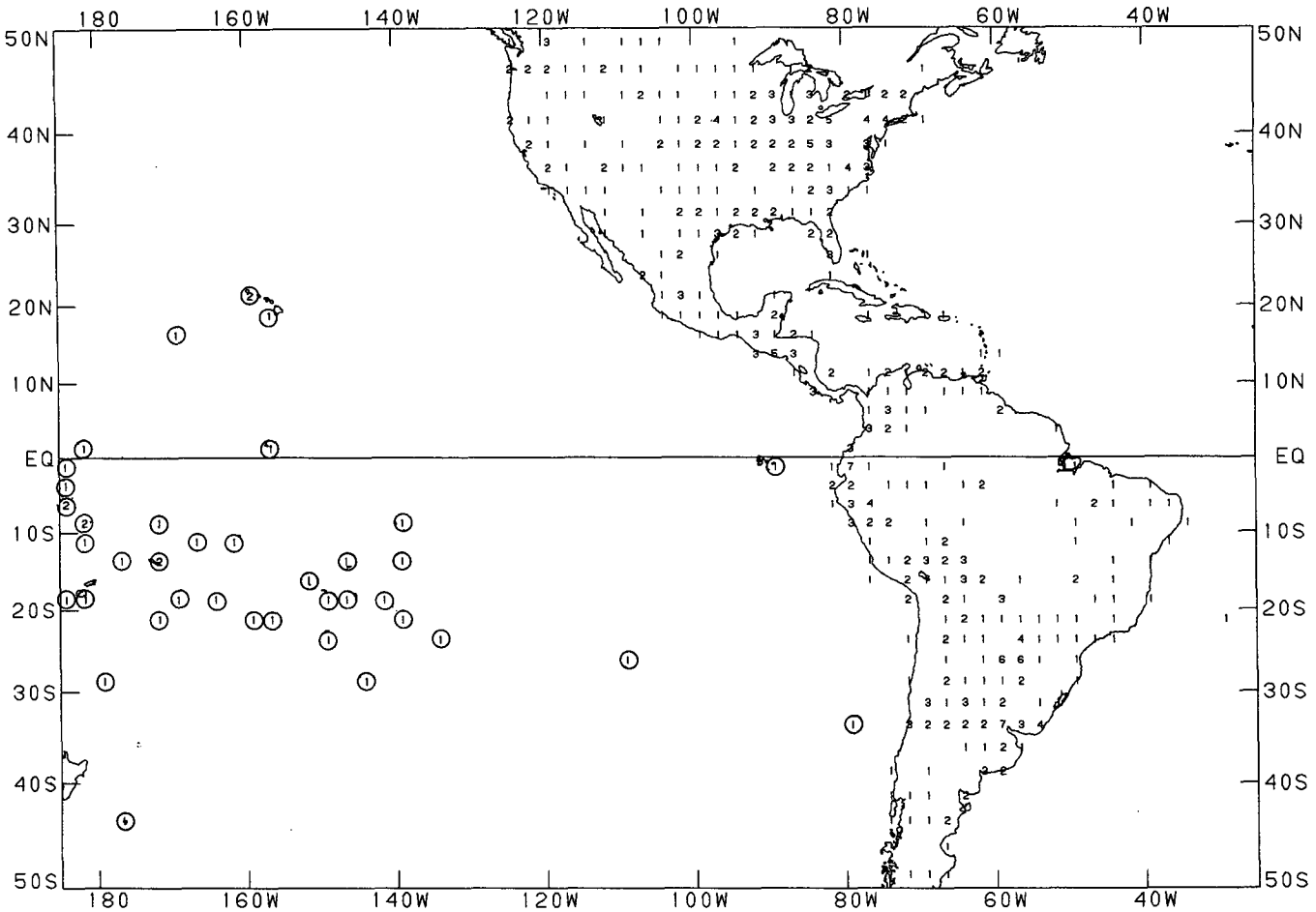

FIG. 6. The number of rainfall observing stations in each 2.5° area used in the comparison of observed rainfall and GPI. The numbers represent the maximum number of stations available in each area for any month during the study period. The numbers representing Pacific Ocean island stations are circled.

available for each CD from January 1931 to December 1984. While the density of reporting stations is not sufficient to completely resolve the spatial variations of convective rainfall, it is considerably greater than that of first-order stations alone.

We analyzed maps of CD rainfall and GPI, as well as spatial and temporal correlations between the two. In order to compute the correlations, rough estimates of observed areal averaged rainfall for any 2.5° box were constructed from the CD data by computing the arithmetic average of all CDs for which the centroid fell within that box. No area weighting was performed. The computation of the GPI was carried out precisely as described in section 2.

The spatial and temporal correlations between the GPI and observed CD rainfall appear to confirm the hypothesis that the GPI is a useful estimate of *convective* rainfall. The pattern correlation (Fig. 8) for the United States south of 40°N exceeds 0.60 for 16 of the 18 months during the warm season (April–September), while only a few of the cold season months reach this value. The temporal correlation for each of the 2.5° boxes over the full 3-yr period is positive over most of the United States (Fig. 9a) and reaches values > 0.70 over Florida, the Mississippi River Valley and the Southwest. However, correlations are much higher when only the months April–September are used (Fig. 9b), with values exceeding 0.75 over much of the area and >0.80 for large parts of the Midwest and Southeast. The slope of the regression between warm season CD rainfall and the GPI (Fig. 10) is close to 1.0 in several coastal regions and, in general, decreases inland. The amount of rain associated with a given areal extent of cold cloud is greater near the coast than inland. This indicates that changes in tropospheric temperature and low-level moisture might be reflected in changes in the coefficient of the linear relationship between areal coverage of cold cloud and rainfall (see Adler and Mack, 1984). Even coastal regions with distinctly low correlations (such as the northwest United States and the

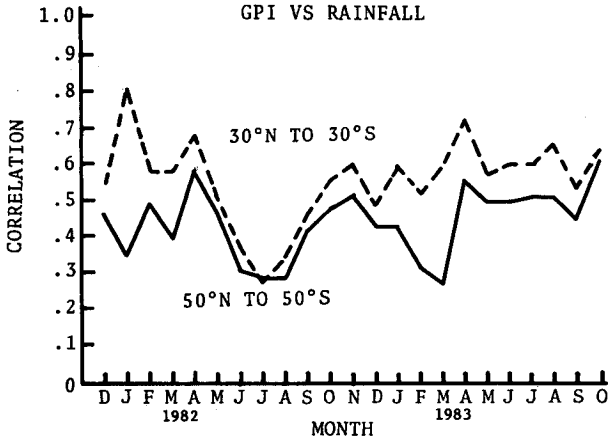

FIG. 7. Time series of the spatial correlation between monthly rainfall observed at the stations identified in Fig. 6 and GPI for the region from 30°N to 30°S and for the entire 50°N to 50°S region.

Carolinas in Fig. 9) exhibit higher correlations than those areas directly inland.

An area where the correlations indicate that the GPI does not accurately reflect the variability of convective rainfall is in the Rocky Mountains. This reinforces the notion that a simple indirect estimation technique such as the GPI is unable to satisfactorily accommodate all the complexities in the cloudiness–rainfall relation in areas of complex terrain.

The difference between the mean GPI and mean CD rainfall taken over the 18 months of the warm seasons (Fig. 11a) gives some indication of the bias of the GPI estimates. Except for a few coastal locations, the GPI exhibits a positive bias across the entire country. Values are relatively small along all coastlines, although this is of little significance in the West, where warm season rainfall is of minor importance. Observed long-term monthly mean warm season rainfall over the United States (Steinhauser, 1979) ranges from >200 mm along the Gulf Coast and over Florida in some months to <50 mm over most of the area west of 100°W. Values > 100 mm are found over extensive portions of the Mississippi River Valley and the eastern United States in many months, and over most of the southeast United States in all months. The ratio of the bias to the observed CD rainfall (Fig. 11b) is <0.2 within about 500 km of the Atlantic and Gulf coasts, and increases to >0.6 west of about 95°W. Comparison of Figs. 9 and 11 show that there is an area west of about 105°W where the correlation between GPI and CD rainfall is quite low and the bias is large compared to the monthly mean. No recalibration of the GPI will yield satisfactory estimates of rainfall in this region; if satellite estimates are necessary, some alternate scheme must be used. In much of the eastern and southeastern portions of the United States, warm season correlations are high and the bias is small; here the current form of the GPI may provide useful estimates of warm season

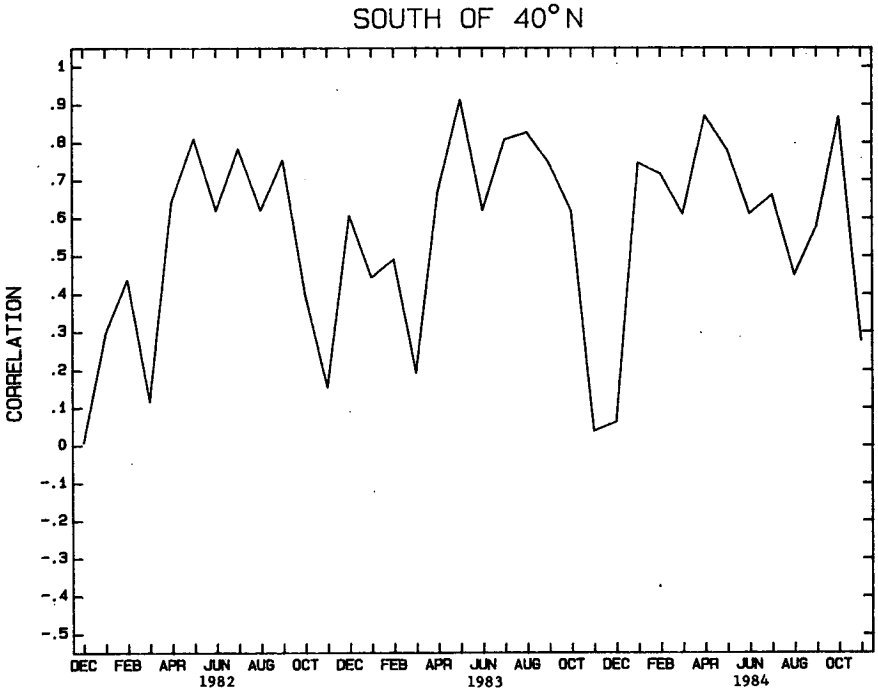

FIG. 8. Time series of the spatial correlation between monthly GPI and Climate Division (CD) rainfall for the United States south of 40°N.

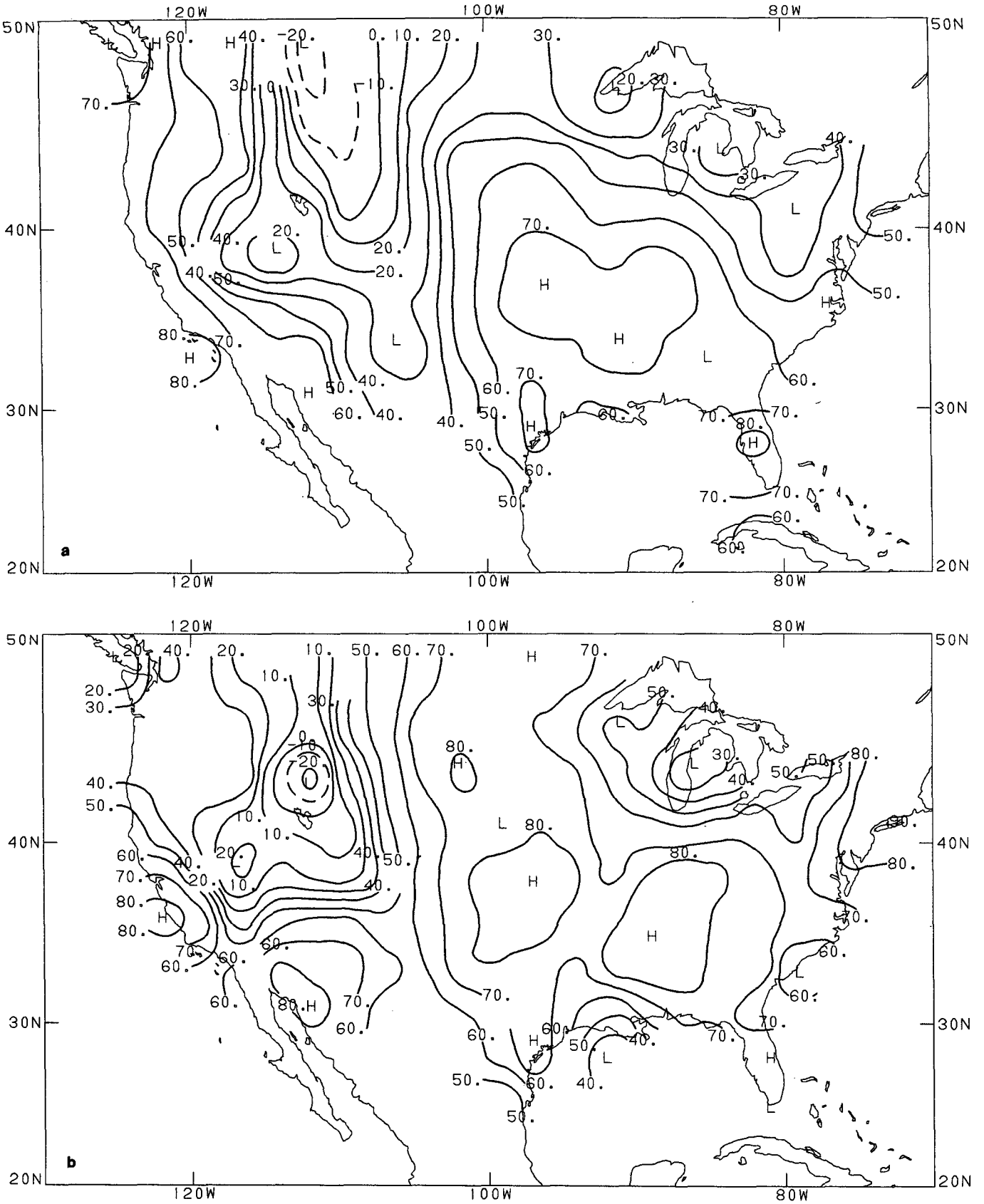

FIG. 9. The temporal correlation (multiplied by 100) between monthly CD rainfall and GPI over (a) the full 3-yr period used in the study and (b) over the warm season (April–September) only. Contour interval is 10, with negative contours dashed.

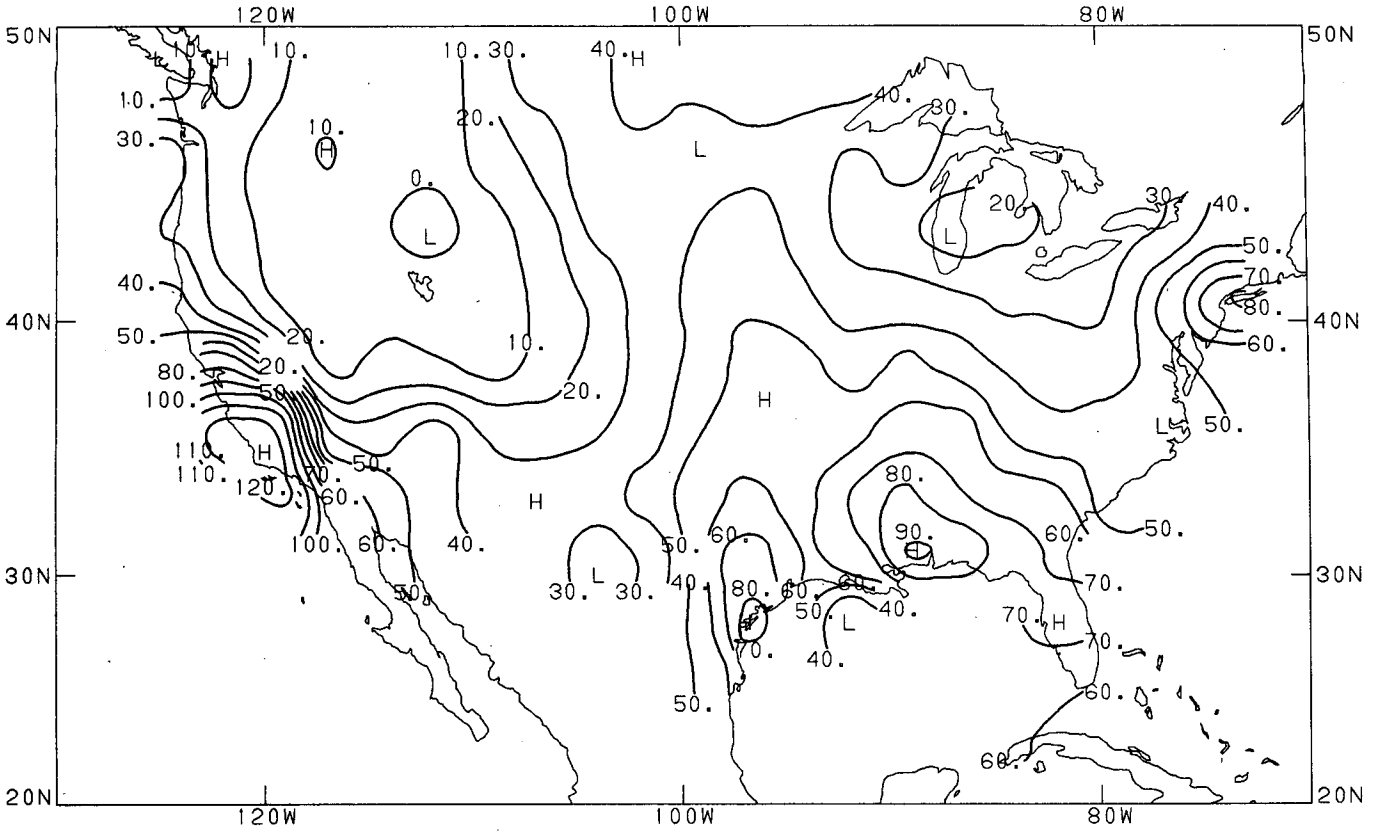

FIG. 10. Slope (multiplied by 100) of the regression between CD rainfall and GPI for the warm season. Contour interval is 10.

rainfall. In between these two areas there is a region where the correlations are high (>0.7), but the bias is also large (50%–150% of the monthly mean CD rainfall). In this region, a useful rainfall estimate might be obtained through a recalibration of the GPI algorithm.

c. *South America*

The ENSO episode of 1982–83 was the most extreme in at least the last 100 years (Rasmusson and Wallace, 1983). ENSO episodes are associated with variations in tropical precipitation in many parts of the globe (Rasmusson and Carpenter, 1983; Kousky et al., 1984). In this section we shall describe the variations in GPI over tropical South America that were associated with the episode and relate them to some of the available station observations.

The 1982–83 ENSO episode began during the northern summer of 1982 and began to strongly affect South America near the end of that year (Quiroz, 1983; Rasmusson and Wallace, 1983). The GPI for the seasons DJF 1981–82, MAM 1982 and JJA 1982 has been subtracted from the GPI for the same season during the following year to obtain an estimate of the interannual change in precipitation associated with the ENSO episode (Figs. 12–14). Three coherent phenomena are seen to dominate the spatial pattern of interannual change in and near tropical South America during this episode: 1) GPI increases in the equatorial eastern Pacific and along the west coast of South America, 2) decreases in the GPI across much of interior Brazil, and 3) increases in the GPI across southern Brazil and Paraguay.

The gradual eastward advance of the main equatorial rainfall maximum has been documented elsewhere (Arkin, 1983; Arkin et al., 1983). Here it can be seen that the principal increases in the eastern Pacific and west coast of South America reached the coast during DJF 1982–83 (Fig. 12). Very large increases were observed in the eastern Pacific during MAM (Fig. 13) and JJA (Fig. 14) of 1983, with the axis of strongest changes slightly south of the equator during MAM and near 4°N during JJA. Local increases of >400 mm relative to the previous year were found in this area during MAM. In each of the three seasons, the increases extended only a short distance inland from the west coast.

A broad area of tropical South America east of the Andes and extending into the equatorial Atlantic exhibited strong decreases in GPI during DJF 1982–83 and MAM 1983 from the year before. The largest de-

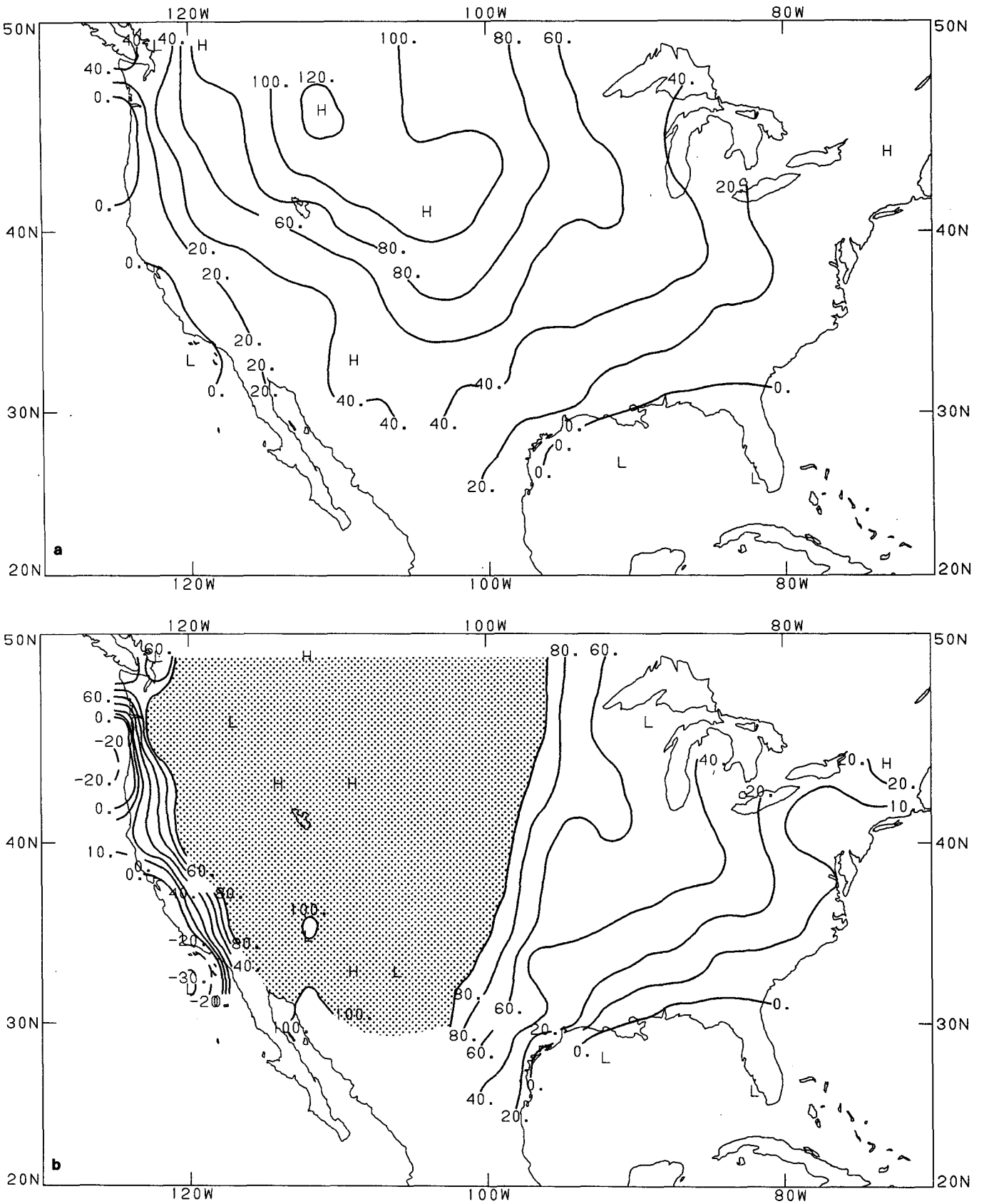

FIG. 11. (a) Monthly mean bias of the GPI relative to the CD rainfall for the warm seasons of 1982–84. Contour interval 20 mm. (b) Ratio (in percent) of the GPI bias to the CD rainfall. Contour interval 20% with an additional contour at 10%. Values > 100% are shaded rather than contoured.

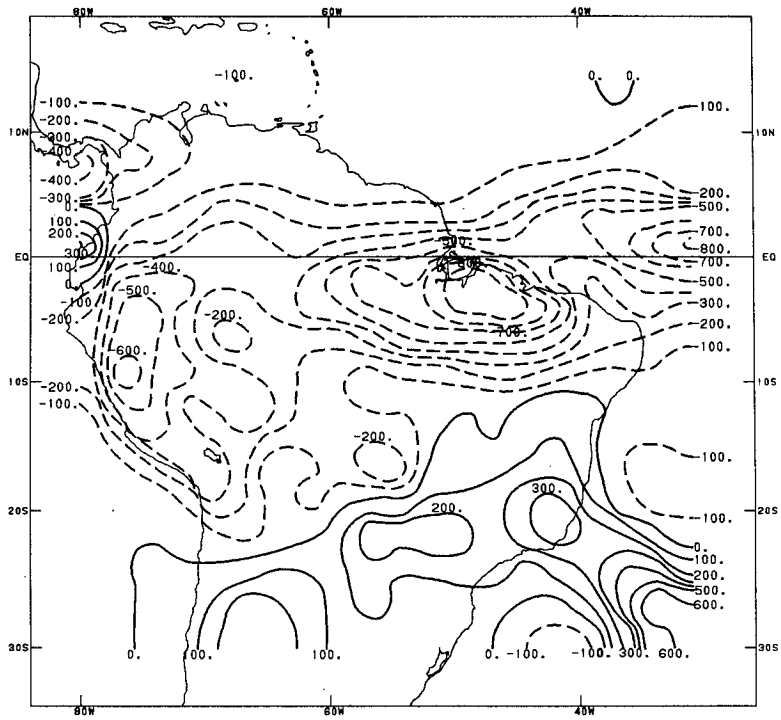

FIG. 12. Difference between DJF 1981–82 and DJF 1982–83 GPI for tropical South America. Increase/decrease from 1981–82 to 1982–83 is positive/negative. Contour interval is 100 mm with negative contours dashed.

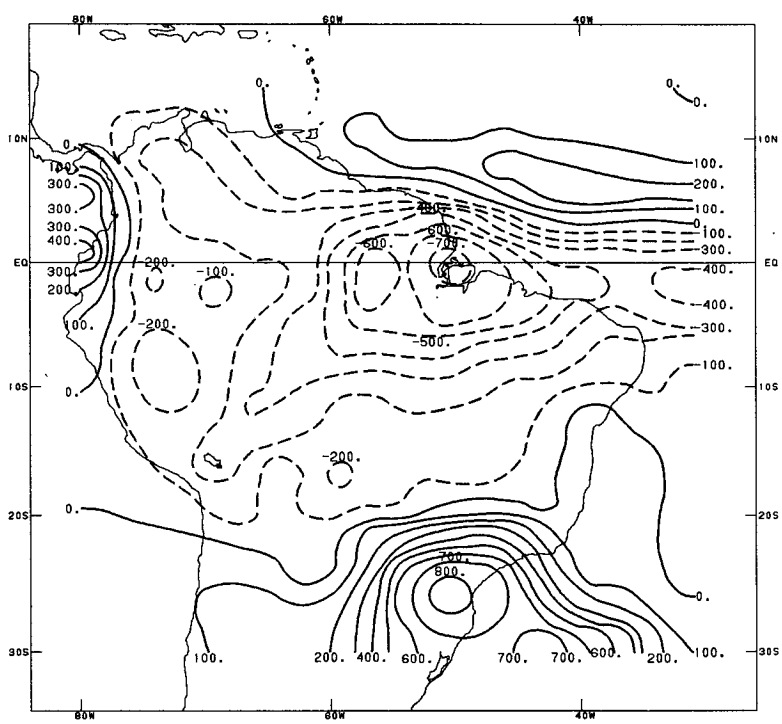

FIG. 13. As in Fig. 12 except for MAM 1982 and MAM 1983.

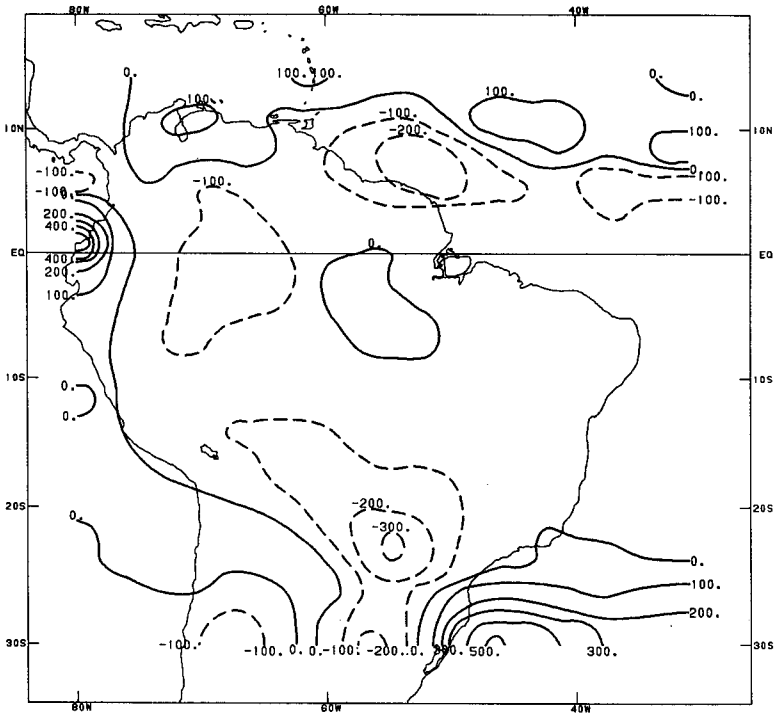

FIG. 14. As in Fig. 12 except for JJA 1982 and JJA 1983.

clines were centered near the mouth of the Amazon in both seasons (Figs. 12, 13). In both seasons, decreases of >200 mm were observed over areas of 10°–15° latitude and 30°–40° longitude. By the JJA 1983 season (Fig. 14), the GPI changes in tropical South America had declined to near zero. This is, to a certain extent, a consequence of the fact that the annual cycle reaches its minimum during this season (see section 3b). However, it is also associated with the decline of the 1982–83 ENSO episode (Ropelewski, 1984, 1985).

Observations of rainfall at a number of stations in tropical Brazil during December 1982–May 1983 and the previous year (obtained from *Monthly Climatic Data for the World*) were differenced to obtain some idea of the accuracy of the GPI-estimated changes. Comparison of changes in seasonal totals at these stations with the corresponding changes in GPI (Figs. 15, 16) indicates that the GPI has successfully captured the general distribution. The changes in GPI, however, are seen to be 1.5–2 times larger than the changes observed at individual stations.

Despite the large decreases in GPI in much of equatorial South America during the 1982–83 ENSO episode, changes in drought-prone Northeast Brazil were quite small. It appears that the small changes in this region resulted from a continuation of a long-term drought rather than from the occurrence of near-normal rainfall. The difference between GPI during MAM 1984 and 1983 (Fig. 17) shows that strong increases were observed during 1984. These were associated with a return to normal or above-normal precipitation (Moura and Kagano, 1986).

Southeastern Paraguay and southern Brazil (40°–60°W, 20°–30°S) exhibited strong increases from MAM 1982 to MAM 1983 (Fig. 13). Somewhat less impressive increases were found in the preceding season. This region is known to have experienced extraordinary flooding and devastation through mid-1983 (Quiroz, 1983; Ropelewski, 1984).

5. Summary and conclusions

In this paper we have briefly reviewed the reasons for and an approach to estimation of large-scale convective precipitation using satellite data. A simple indirect technique, using the fraction of 2.5° × 2.5° areas covered by pixels (picture elements) with EBBT < 235 K in geostationary IR imagery together with the linear relationship derived by Richards and Arkin (1981) for the GATE A/B array, was applied to data from the United States geostationary satellites beginning in December 1981. The derived estimates (the GOES Precipitation Index—GPI) were used to describe the 3-yr mean annual cycle in estimated rainfall and to compare it to published estimates of the long-term mean annual cycle. Year-to-year changes in GPI were then compared to changes in station observations of rainfall over the United States and tropical South America.

The spatial distribution and evolution of the GPI through the annual cycle appears quite realistic in

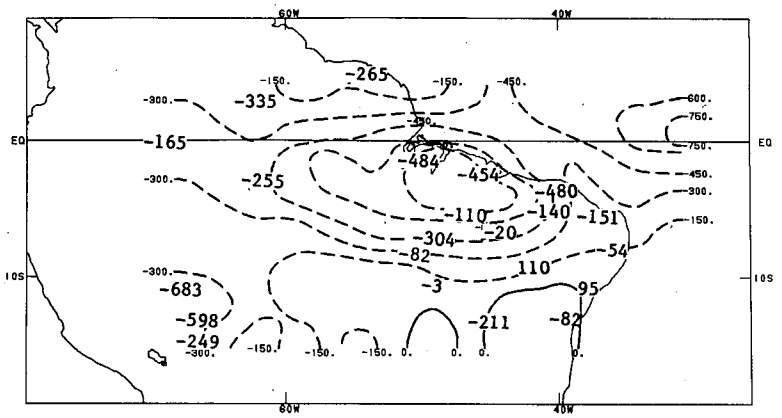

FIG. 15. Portion of Fig. 12 from 5°N to 15°S with interannual change (for DJF) at individual stations plotted (large numerals).

comparison with published climatologies. The GPI amounts were within the range of those published over the tropical oceans. Considering the difficulty in obtaining accurate estimates of areal averaged oceanic precipitation from any source, it appears that the GPI might prove most valuable in the measurement of tropical oceanic rainfall. Over North and South America, the placement and seasonal changes in GPI extrema through the annual cycle closely resembled those found in the long-term mean. Individual peak values were not greatly different, but the areally integrated values of GPI exceeded those of rainfall during the rainy season. This is believed to be at least partially due to the fact that the areal extent of values > 300 mm/month was substantially greater in GPI over South America during months of heavy rainfall than in the published climatologies. In contrast, the coverage of amounts > 100 mm/month was not very different.

Comparison of GPI with observations of rainfall for the 3-yr period confirmed the results of Arkin (1979) and Richards and Arkin (1981). Tropical convective rainfall was best estimated using a threshold of 235 K, while in the extratropics a threshold of 220 K was best. The lower threshold was significantly better at discriminating convective and nonconvective cloud at higher latitudes. The GPI in both the United States and tropical South America successfully represented the interannual variability found in observed convective rainfall, although the amplitude of GPI changes appeared to be somewhat higher than that of changes in observed rainfall.

Several conclusions may be drawn from these results:

1) the linear relationship between fractional coverage of cold cloud and rainfall obtained by Arkin (1979) and Richards and Arkin (1981) for the GATE area is at least approximately valid in other convective regions;

2) the GPI is successful at documenting the spatial and temporal variability in convective regimes with greater detail than is possible using station data alone;

3) estimation of actual rainfall over continental regions with this simple statistical technique requires local calibration of the quantitative relationship between coverage of cold cloud and rainfall;

4) the GPI probably provides a better estimate of

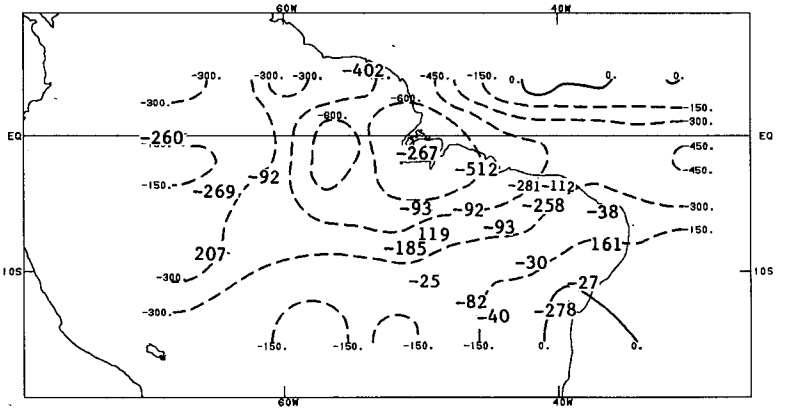

FIG. 16. As in Fig. 15 except derived from Fig. 13 (MAM).

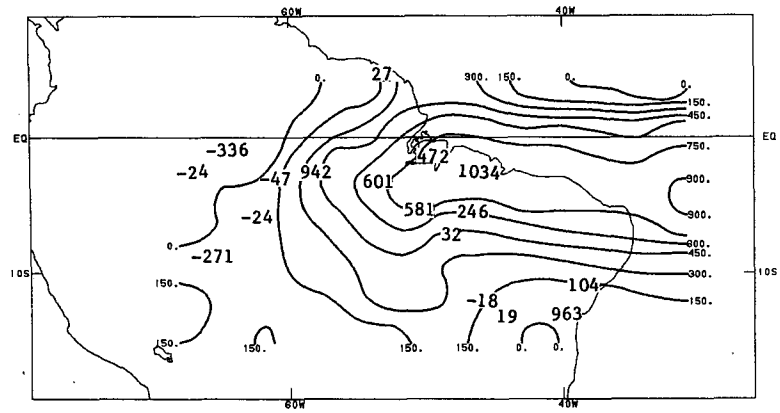

FIG. 17. Difference in GPI between MAM 1983 and MAM 1984 (contours) along with the difference between the same seasons at individual stations (large numerals). Increase from 1983 to 1984 is positive. Contour interval is 150 mm; plotted station values are in millimeters.

tropical ocean rainfall for individual months and years than has ever been available from any source.

It is evident that two activities would, if pursued, have great potential for climate studies. Firstly, the statistical relationship between rainfall and coverage by cold cloud should be better documented in both space and time. The obvious method would be the conduction of a number of calibration studies in which detailed observations of the areally averaged rainfall for a variety of areas and times of year would be compared to statistics of the cloud population as in Richards and Arkin (1981). Secondly, the spatial coverage of GPI-like estimates of convective rainfall could be expanded to cover the vast majority of the convective regions of the world by the acquisition of suitable statistics from all operating geostationary satellites. These estimates provide an initial solution to the problem of obtaining measurements of tropical oceanic rainfall for the Tropical Ocean/Global Atmosphere Program of the World Climate Research Program (WCRP, 1985).

Acknowledgments. We are grateful to John Kopman for his assistance in drafting some of the figures; to Gail Lucas, Dottie Vanderbrink and Kathy Stevenson for helping to prepare the manuscript; and to Gene Rasmusson, Chet Ropelewski, Vern Kousky, Yale Mintz and Cecelia Griffith for interesting discussions and comments on earlier versions of the paper. John Moses provided us with an exceptionally thorough and helpful review.

REFERENCES

Adler, R. F., and R. A. Mack, 1984: Thunderstorm cloud height–rainfall rate relations for use with satellite rainfall estimation techniques. *J. Climate Appl. Meteor.*, **23,** 280–296.

Arkin, P. A., 1979: The relationship between fractional coverage of high cloud and rainfall accumulations during GATE over the B-scale array. *Mon. Wea. Rev.*, **107,** 1382–1387.

——, 1983: Tropical circulation anomalies associated with the 1982–83 ENSO event. *Proc. Eighth Climate Diagnostics Workshop,* Toronto, 111–121.

——, J. D. Kopman and R. W. Reynolds, 1983: *The 1982–83 El Niño/Southern Oscillation Event Quick Look Atlas.* Available from the Climate Analysis Center, W/NMC52, NWS/NOAA, Washington, DC 20233.

Barrett, E. C., 1970: The estimation of monthly rainfall from satellite data. *Mon. Wea. Rev.*, **98,** 322–327.

——, and D. W. Martin, 1981: *The Use of Satellite Data in Rainfall Monitoring.* Academic Press, 340 pp.

Clark, D., 1983: *The GOES User's Guide.* National Environmental Satellite and Data Information Service, Washington, DC, 163 pp.

Dorman, C. E., and R. H. Bourke, 1978: A temperature correction for Tucker's ocean rainfall estimates. *Quart. J. Roy. Meteor. Soc.*, **104,** 756–773.

——, and ——, 1979: Precipitation over the Pacific Ocean, 30°S to 60°N. *Mon. Wea. Rev.*, **107,** 896–910.

——, and ——, 1981: Precipitation over the Atlantic Ocean, 30°S to 70°N. *Mon. Wea. Rev.*, **109,** 554–563.

Garcia, O., 1981: A comparison of two satellite rainfall estimates for GATE. *J. Appl. Meteor.*, **20,** 430–438.

Griffith, C. G., W. L. Woodley, J. S. Griffin and S. C. Stromatt, 1980: *Satellite-Derived Precipitation Atlas for GATE.* NOAA Atlas Series, Environmental Research Laboratories, Boulder, CO, 280 pp. [Superintendent of Documents, No. 0-315-309].

——, ——, P. G. Grube, D. W. Martin, J. Stout and D. N. Sikdar, 1978: Rain estimation from geosynchronous satellite imagery—visible and infrared studies. *Mon. Wea. Rev.*, **106,** 1153–1171.

Hoffman, J. A. J., 1975: *Climatic Atlas of South America.* WMO, 41 Avenue Giuseppe-Motta, Geneva, 4 pp. + 28 Fig.

Horel, J. D., and J. M. Wallace, 1981: Planetary-scale atmospheric phenomena associated with the Southern Oscillation. *Mon. Wea. Rev.*, **109,** 813–829.

Hudlow, M. D., 1979: Mean rainfall patterns for the three phases of GATE. *J. Appl. Meteor.*, **18,** 1656–1669.

——, and V. L. Patterson, 1979: *GATE Radar Rainfall Atlas.* NOAA Special Report, Environmental Data and Information Service, Washington, DC, 155 pp. [Superintendent of Documents, No. 003-19-0046-2].

——, R. K. Farnsworth and D. R. Greene, 1981: Hydrologic forecasting requirements for precipitation data from space measurements. *Precipitation Measurements from Space—Workshop Report,* NASA, Goddard Space Flight Center, Greenbelt, MD, D23–D30.

Jaeger, L., 1976: Monatskarten des Niederschlags fur die ganze Erde. *Berichte des Deutschen Wetterdienstes,* Nr. 139 (Band 18). Offenbach A.M., 33 pp. and plates.

Kilonsky, B. J., and C. S. Ramage, 1976: A technique for estimating tropical open-ocean rainfall from satellite observations. *J. Appl. Meteor.,* **15,** 972–975.

Kousky, V. E., M. T. Kagano and I. F. A. Cavalcanti, 1984: A review of the Southern Oscillation: Oceanic–atmospheric circulation changes and related rainfall anomalies. *Tellus,* **36A,** 490–504.

Mintz, Y., 1981: A brief review of the present status of global precipitation measurements. *Precipitation Measurements from Space—Workshop Report,* NASA, Goddard Space Flight Center, Greenbelt, MD, D1–D4.

Moura, A., and M. T. Kagano, 1986: Large-scale precipitation variations over South America during the ENSO event 1982–83. *Proc. First WMO Workshop on the Diagnosis and Prediction of Monthly and Seasonal Atmospheric Variations over the Globe,* College Park, MD, 217–224.

Negri, A. J., R. F. Adler and P. J. Wetzel, 1984: Rainfall estimation from satellites: An examination of the Griffith–Woodley technique. *J. Climate Appl. Meteor.,* **23,** 102–116.

Quiroz, R. S., 1983: The climate of the "El Niño" winter of 1982–83—A season of extraordinary climatic anomalies. *Mon. Wea. Rev.,* **111,** 1686–1706.

Rasmusson, E. M., and P. A. Arkin, 1981: Precipitation data for climate diagnostics. *Precipitation Measurements from Space—Workshop Report,* NASA, Goddard Space Flight Center, Greenbelt, MD, D10–D18.

——, and T. H. Carpenter, 1982: Variations in tropical sea surface temperature and surface wind fields associated with the Southern Oscillation/El Niño. *Mon. Wea. Rev.,* **110,** 534–584.

——, and ——, 1983: The relationship between eastern equatorial Pacific sea surface temperatures and rainfall over India and Sri Lanka. *Mon. Wea. Rev.,* **111,** 517–528.

——, and J. M. Wallace, 1983: Meteorological aspects of the El Niño/Southern Oscillation. *Science,* **222,** 1195–1202.

——, P. A. Arkin, W. Y. Chen and J. B. Jalickee, 1981: Biennial variations in surface temperature over the United States as revealed by singular decomposition. *Mon. Wea. Rev.,* **109,** 587–598.

Richards, F., and P. Arkin, 1981: On the relationship between satellite-observed cloud cover and precipitation. *Mon. Wea. Rev.,* **109,** 1081–1093.

Ropelewski, C. F., 1984: The climate of summer 1983—a season of contrasts and extremes. *Mon. Wea. Rev.,* **112,** 591–609.

——, 1985: The global climate June–August 1984: A return to "normal" in the tropics. *Mon. Wea. Rev.,* **113,** 664–679.

Steinhauser, F., 1979: *Climatic Atlas of North and Central America.* WMO, 41 Avenue Giuseppe-Motta, Geneva, 8 pp. + 28 Fig.

Strommen, N. D., R. F. Dale and E. P. Motha, 1981: Agricultural requirements for precipitation measurements. *Precipitation Measurements from Space—Workshop Report,* NASA, Goddard Space Flight Center, Greenbelt, MD, D19–D22.

Trenberth, K. E., 1976: Spatial and temporal variations of the Southern Oscillation. *Quart. J. Roy. Meteor. Soc.,* **102,** 639–653.

Tucker, G. G., 1961: Precipitation over the North Atlantic Ocean. *Quart. J. Roy. Meteor. Soc.,* **87,** 147–158.

WCRP, 1985: *Scientific Plan for the Tropical Ocean and Global Atmosphere Programme.* TOGA Scientific Steering Group, WCRP Pub. Series No. 3, Geneva, 147 pp.

Wilheit, T. T., A. T. Chang, M. S. V. Rao, E. B. Rodgers and J. S. Theon, 1977: A satellite technique for quantitatively mapping rainfall rates over the ocean. *J. Appl. Meteor.,* **16,** 551–560.